



# New Ethenzamide-Trimesic Acid Cocrystal: Equilibrium Solubility

Shuting Lin, Jiarong Zhang, Weijie Sun, Penghui Ren, Jiayi Jiang, Chengjun Jiang\*

School of Biological and Chemical Engineering, Zhejiang University of Science and Technology, Hangzhou, China

Email: \*jcj312@zust.edu.cn

**How to cite this paper:** Lin, S.T., Zhang, J.R., Sun, W.J., Ren, P.H., Jiang, J.Y. and Jiang, C.J. (2023) New Ethenzamide-Trimesic Acid Cocrystal: Equilibrium Solubility. *Open Access Library Journal*, **10**: e10247. <https://doi.org/10.4236/oalib.1110247>

**Received:** May 12, 2023

**Accepted:** June 16, 2023

**Published:** June 19, 2023

Copyright © 2023 by author(s) and Open Access Library Inc.

This work is licensed under the Creative Commons Attribution International License (CC BY 4.0).

<http://creativecommons.org/licenses/by/4.0/>



Open Access

## Abstract

Ethenzamide, a non-steroidal anti-inflammatory drug, is used to treat pain, inflammation, fever and rheumatism. However, it has low solubility and belongs to class II of the biopharmaceutical classification system. In order to improve the solubility of ethenzamide, the cocrystal of ethenzamide was prepared and characterized according to the synthesis principle of hydrogen bond supramolecular synthons in crystal engineering. The ETZ·2TMA·MeOH cocrystal was obtained by the solution evaporation crystallization method. The cocrystal structure was characterized by Single Crystal X-ray Diffractometer. The single crystal belongs to orthorhombic crystal system with space group  $P2_12_12_1$  (no.19),  $a = 12.9863$  (9) Å,  $b = 16.6603$  (11) Å,  $c = 25.9260$  (16) Å,  $V = 5609.2$  (6) Å<sup>3</sup>,  $Z = 8$ ,  $T = 170.00$  K. The main forces are the formation of intermolecular hydrogen bonds between the amide groups on ethenzamide and the carboxyl groups on trimesic acid and the hydroxyl group on methanol. In addition, the solubility of ethenzamide and ETZ·2TMA·MeOH cocrystal was determined. The results show that, in contrast to most cocrystal systems that improve solubility, the solubility of ETZ·2TMA·MeOH decreased to 19.30% of pure ethenzamide.

## Subject Areas

Chemical Engineering and Technology

## Keywords

Pharmaceutical, Cocrystal, Ethenzamide, Crystal Engineering, Solubility

## 1. Introduction

Ethenzamide (CAS: 938-73-8, 2-ethoxybenzamide, ETZ) is a non-steroidal anti-inflammatory drug with analgesic and antipyretic effects [1]. It can be used to

treat mild to moderate pain in muscle, bone and joint diseases. ETZ belongs to class II of Biological drug Classification System (BCS), and its main disadvantages are poor solubility and low bioavailability [2]. The structures of cocrystal of ETZ have been published and deposited in CSD (Cambridge Structural Database), which was obtained with furosemide (CCDC: 2,114,160, SARQOV) [3], sinapic acid (CCDC: 1,581,650, DEYQUW) [4], 2,5-dihydroxybenzoic acid (CCDC: 1,522,933, FENQEX), 3,4-dihydroxybenzoic acid (CCDC: 1,522,937, FENRIC) [5], phenol (CCDC: 1,879,336, VUKSEC) [6], 3,5-dinitrobenzoic acid (CCDC: 752,467, WUZHOP) [7], 2,4-dihydroxybenzoic acid (CCDC: 1,825,011, JIFHAK) [8], 3,4,5-trihydroxybenzoic acid (CCDC: 1,468,148, ORIKIL), 2-nitro-benzoic acid (CCDC: 1,468,153, ORIKOR), 3-nitrobenzoic acid (CCDC: 1,468,154, ORIKUX), 2,4-dinitrobenzoic acid (CCDC: 1,468,159, ORILAE), 3-methylbenzoic acid (CCDC: 1,468,161, ORILEI) [9], 2-hydroxybenzoic acid (CCDC: 752,480, REHSAA) [10], pentanedioic acid (CCDC: 1,854,255, TIWPIB) [11], (2Z)-but-2-enedioic acid (CCDC: 1,854,256, TIWPOH) [11], Flufenamic Acid (CCDC: 1,448,786, FAQXAZ) [12], Ferulic acid (CCDC: 1,448,786, FAQXAZ) [13], propanedioic acid (CCDC: 1,854,257, TIWPUN) [11], ethylmalonic acid (CCDC: 752,465, VAKTOS) [2], Saccharin (CCDC: 711,674, VUHFIO) [14] and so on.

Different cocrystals can cause different trend of solubilities. For example, ETZ·3,5-dinitrobenzoic acid ( $19.47 \text{ mg}\cdot\text{mL}^{-1}$ ), ETZ·2,4-dihydroxybenzoic acid ( $4.78 \text{ mg}\cdot\text{mL}^{-1}$ ) improved the solubility of ETZ ( $1.45 \text{ mg}\cdot\text{mL}^{-1}$ ), while ETZ·ferulic acid ( $1.15 \text{ mg}\cdot\text{mL}^{-1}$ ) reduced the solubility of ETZ ( $1.45 \text{ mg}\cdot\text{mL}^{-1}$ ). In this research, we discovered the cocrystal of ETZ·2TMA·MeOH, which laid a foundation for the further study of ETZ new cocrystal.

## 2. Experimental

### 2.1. Materials

Ethenzamide (Energy Chemical Co., Ltd., China), Trimesic acid (TMA) (Energy Chemical Co., Ltd., China), Methanol (Shanghai Lingfeng Chemical Reagent Co., Ltd., China) and toluene (Shanghai Lingfeng Chemical Reagent Co., Ltd., China).

### 2.2. Tools and Equipment

Fourier Transform-Infrared Spectroscopy (FT-IR) (VERTEX 70, Bruker, America), Powder X-Ray Diffraction (PXRD) (Rigaku, Tokyo, Japan), Single Crystal X-Ray diffraction (SXRD) (Bruker APEX-II, Bruker, America), High-performance Liquid Chromatography (HPLC) (Waters-e2695, Waters, America).

### 2.3. Cocrystal Growth

Equimolar quantities of ETZ (0.20 mol) and TMA (0.20 mol) were added to a mixed solvent of 2 mL of methanol and 3 mL of toluene in a 10 mL glass vial. The slurry was stirred at  $60^\circ\text{C}$  for 10 min. The obtained clear solution was

cooled down slowly to room temperature for 2 days.

#### 2.4. Fourier Transform-Infrared Spectroscopy (FT-IR)

The infrared spectra of samples were evaluated by an FT-IR spectrometer (Bruker Alpha FT-IR spectrometer). The measurements were performed in a range of 4000 - 400  $\text{cm}^{-1}$  with a resolution of 4  $\text{cm}^{-1}$ . Powder samples (about 2 mg) were manually mixed with 100 mg of dry KBr in an agate mortar and pressed into thin pellets. Data were analyzed by Spectrum software.

#### 2.5. Powder X-Ray Diffraction (PXRD)

The diffraction patterns were measured on Rigaku Ultima IV X-ray Diffractometer (Rigaku, Tokyo, Japan) using Cu  $K\alpha$  X-ray ( $\lambda = 1.5406 \text{ \AA}$ ) and the generator operating at 40 kV and 40 mA. The scans ran from  $5.0^\circ$  to  $50.0^\circ$  ( $2\theta$ ), with an increasing step size of  $0.02^\circ$  and a scan rate of  $5^\circ \text{ min}^{-1}$ .

#### 2.6. Single Crystal X-Ray Diffraction (SXRD)

A single crystal of suitable size and good quality was measured by using an area detector on a Bruker APEX-II CCD diffractometer with graphite monochromatic Ga- $K\alpha$  radiation ( $\lambda = 1.34138 \text{ \AA}$ ). Absorption corrections were applied by using a multi-scan program. Using Olex2, the structure was solved with the ShelXT structure solution program using Intrinsic Phasing and refined with the ShelXL refinement package using Least Squares minimization.

#### 2.7. Solubility and Dissolution Studies

The dissolution studies of ETZ and ETA·2TMA·MeOH were measured by using equal molar samples at  $37^\circ\text{C}$  for oscillation. Aliquots of 1 mL were withdrawn at predetermined time points (5, 10, 15, 30, 45, 60, 120, 180, 240 and 1380 min) substituting the same with an equal quantity of fresh dissolution media.

The solubility and dissolution rate of ETZ and ETA·2TMA·MeOH were quantified by High Performance Liquid Chromatography. A Waters e2695 series HPLC equipped with a UV detector (2489) and an automated injector. Methanol-water (80:20) was used as mobile phase at a flow rate of  $1 \text{ mL}\cdot\text{min}^{-1}$  in an isocratic mode on an Agilent Zorbax SB-C18 (4.6 mm  $\times$  250 mm, 5  $\mu\text{m}$ ) column at  $25^\circ\text{C}$ . After suitable dilution, 10  $\mu\text{L}$  of the sample was injected, and the absorbance of elute was recorded at 235 nm.

#### 2.8. Hirshfeld Surface Analysis

Both the Hirshfeld surface image and 2D fingerprint are generated by Crystal Explorer software.

### 3. Results and Discussion

#### 3.1. Solid State X-Ray Crystal Structure Analysis

The ETZ·2TMA·MeOH cocrystal was obtained from a mixed solvent of methanol

and toluene at room temperature by the solvent evaporation method. The single crystal belongs to the orthorhombic crystal system with space group  $P2_12_12_1$  (**Table 1**). In the unit cell of the cocrystal, the main forces are the formation of intermolecular hydrogen bonds between the amide groups on ETZ and the carboxyl groups on TMA and the hydroxyl group on methanol (**Figure 1** and **Table 2**).

**Table 1.** ETA·2TMA·MeOH cocrystal crystallography and refinement data.

	ETA·2TMA·MeOH
Empirical formula	C <sub>28</sub> H <sub>27</sub> NO <sub>15</sub>
Formula weight	617.50
Temperature/K	170.00
Crystal system	orthorhombic
Space group	P2 <sub>1</sub> 2 <sub>1</sub> 2 <sub>1</sub>
a/Å	12.9863 (9)
b/Å	16.6603 (11)
c/Å	25.9260 (16)
$\alpha$ /°	90
$\beta$ /°	90
$\gamma$ /°	90
Volume/Å <sup>3</sup>	5609.2 (6)
Z	8
$\rho_{\text{calc}}$ /cm <sup>3</sup>	1.462
$\mu$ /mm <sup>-1</sup>	0.660
F (000)	2576.0
Crystal size/mm <sup>3</sup>	0.08 × 0.06 × 0.03
Radiation	GaK $\alpha$ ( $\lambda$ = 1.34138)
2 $\Theta$ range for data collection/°	5.486 to 114.53
Index ranges	-16 ≤ h ≤ 15, -20 ≤ k ≤ 20, -31 ≤ l ≤ 32
Reflections collected	42,349
Independent reflections	11,301 [R <sub>int</sub> = 0.0518, R <sub>sigma</sub> = 0.0557]
Data/restraints/parameters	11,301/7/821
Goodness-of-fit on F <sup>2</sup>	1.044
Final R indexes [I ≥ 2 $\sigma$ (I)]	R <sub>1</sub> = 0.0525, wR <sub>2</sub> = 0.1223
Final R indexes [all data]	R <sub>1</sub> = 0.0900, wR <sub>2</sub> = 0.1462
Largest diff. peak/hole/e Å <sup>-3</sup>	0.21/-0.31
Flack parameter	0.03 (11)

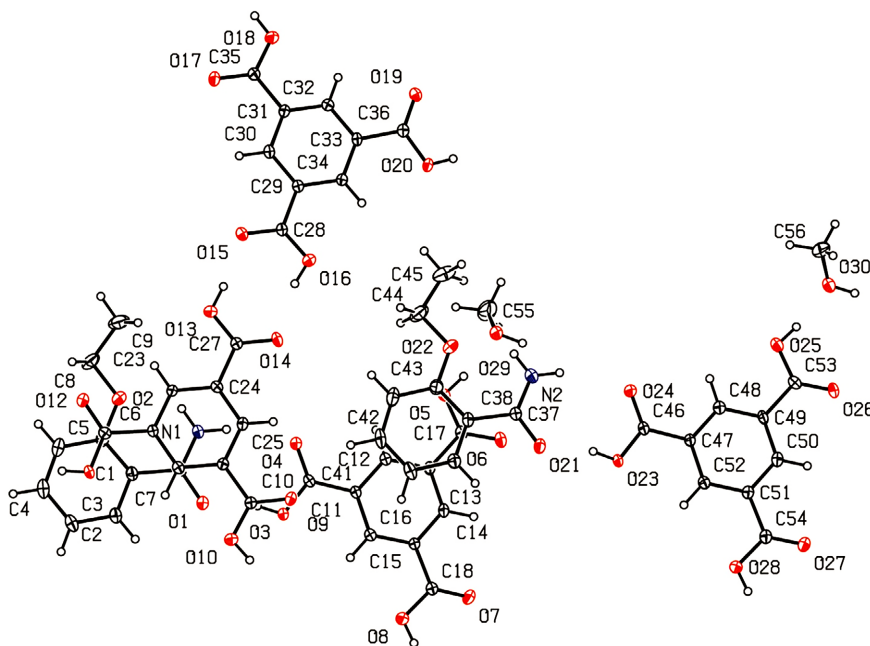


**Figure 1.** Cocrystallization of ETA·2TMA·MeOH.

**Table 2.** ETA·2TMA·MeOH cocrystalline hydrogen bonds.

D	H	A	$d(D-H)/\text{\AA}$	$d(H-A)/\text{\AA}$	$d(D-A)/\text{\AA}$	$D-H-A/^\circ$
N1	H1B	O2	0.88	1.97	2.654 (4)	133.5
O3	H3A	O1	0.84	1.70	2.523 (4)	165.4
O5	H5A	O29	0.84	1.68	2.515 (4)	170.2
O8	H8	O24 <sup>1</sup>	0.84	1.89	2.725 (4)	172.1
O11	H11	O26 <sup>2</sup>	0.84	1.85	2.664 (4)	161.3
O20	H20	O6 <sup>3</sup>	0.84	1.82	2.636 (4)	162.9
N2	H2B	O22	0.88	1.98	2.663 (5)	133.0
O23	H23A	O21	0.84	1.69	2.511 (4)	165.0
O25	H25A	O30	0.84	1.68	2.510 (4)	171.6
O28	H28	O4 <sup>1</sup>	0.84	1.91	2.739 (4)	171.0
O30	H30A	O12 <sup>4</sup>	0.84	1.82	2.655 (4)	171.6
O10	H10	O17 <sup>5</sup>	0.87 (3)	1.81 (3)	2.674 (4)	171 (9)
O13	H13	O15	0.88 (3)	1.73 (3)	2.596 (4)	172 (8)
O16	H16A	O14	0.86 (3)	1.82 (3)	2.662 (4)	165 (8)
O18	H18	O9 <sup>6</sup>	0.87 (3)	1.72 (3)	2.590 (4)	177 (9)
O29	H29	O19 <sup>1</sup>	0.87 (3)	1.79 (3)	2.644 (4)	168 (7)

<sup>1</sup>1 - X, -1/2 + Y, -1/2 - Z; <sup>2</sup>+X, +Y, 1 + Z; <sup>3</sup>1 - X, 1/2 + Y, -1/2 - Z; <sup>4</sup>+X, +Y, -1 + Z; <sup>5</sup>+X, -1 + Y, +Z; <sup>6</sup>+X, 1 + Y, +Z.

On the one hand, the O atom on the amide group of the ETZ molecule is a hydrogen bond acceptor, and the H atom on the carboxyl group (O-H) of the TMA molecule is a hydrogen bond donor, forming an intermolecular hydrogen bond O-H...O (symmetry code: +X, +Y, -1 + Z) [length 2.523 (4) Å, angle 165.4°]. On the other hand, the O atom on the hydroxyl group of the methanol molecule is a hydrogen bond acceptor, and the H atom on the molecular carboxyl group (O-H) of the ETZ molecule is a hydrogen bond donor, forming an intermolecular hydrogen bond O-H...O (symmetry code: +X, +Y, -1 + Z) [length 2.515 (4) Å, angle 170.2°]. The methanolate cocrystal of ETZ and TMA were formed. Views of the calculated ETA·2TMA·MeOH Hirshfeld surface and 2D fingerprint were shown in **Figure 2**. The force of H... O/O... H is 34.5%, and the force of H... N/N... H is 0.7%. The force of the hydrogen bond between ETZ and TMA mainly depends on H... O/O... H force.

### 3.2. PXRD Analysis

The crystal structures of ETZ, TMA, and ETA·2TMA·MeOH were measured by PXRD (**Figure 3**). The peaks at  $2\theta = 9.64^\circ$ ,  $14.54^\circ$ ,  $14.70^\circ$ ,  $19.36^\circ$ ,  $25.32^\circ$ , and  $33.78^\circ$ , which are the characteristic peaks of ETZ, disappeared in the PXRD result of ETA·2TMA·MeOH. Meanwhile, a number of new peaks belonging to ETA·2TMA·MeOH emerged at  $2\theta = 26.84^\circ$ . Thus, the formation of ETA·2TMA·MeOH can be confirmed by the notable changes through the PXRD.

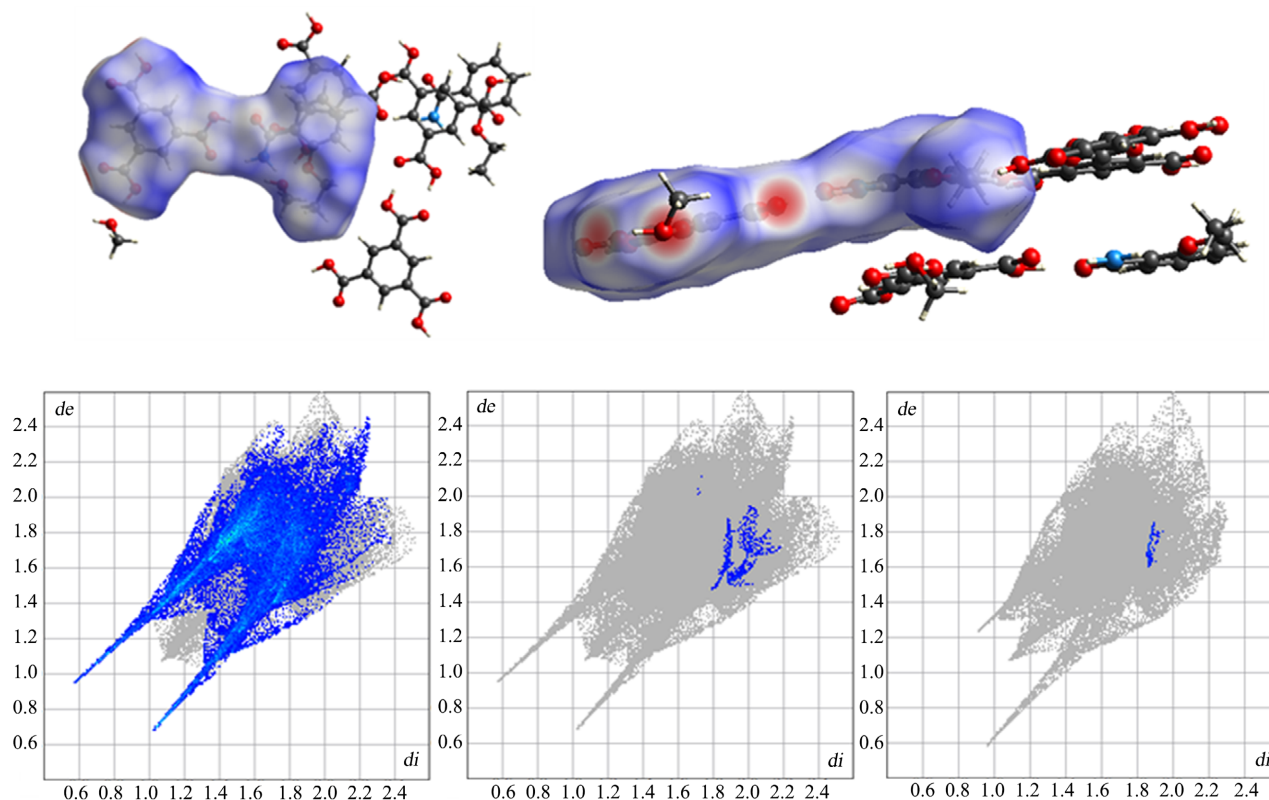


**Figure 2.** Views of the calculated ETA·2TMA·MeOH Hirshfeld surface.

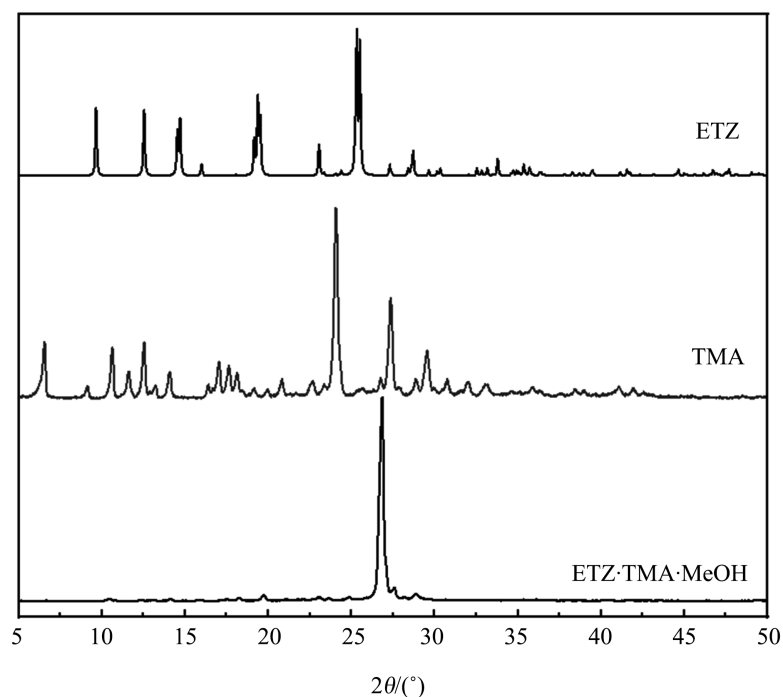


**Figure 3.** The powder X-ray diffraction (PXRD) patterns of ETZ, TMA and ETA-2TMA·MeOH.

### 3.3. FT-IR Analysis

The synthesized ETA-2TMA·MeOH was analyzed by FT-IR spectroscopy. FT-IR spectra of ETZ, TMA and ETA-2TMA·MeOH were compared in order to confirm the cocrystal formation. All the molecular cocrystals exhibited a change in the carbonyl stretching frequency of the acid group with respect to their starting material.

In the ETA-2TMA·MeOH, a significant shift of carboxylate ( $\text{-C=O}$ ) and amino ( $\text{-NH}_2$ ) stretching vibration was observed (Figure 4). The characteristic peak of N-H in the molecular structure of ETZ was shifted from  $3370.51\text{ cm}^{-1}$  to  $3453.93\text{ cm}^{-1}$ , the characteristic absorption peak of C=O in the molecular structure of TMA was shift from  $1644.27\text{ cm}^{-1}$  to  $1705.51\text{ cm}^{-1}$ .

### 3.4. Solubility Study

It is well known that the solid form of APIs has a substantial impact on the solubility and dissolution profiles of drug. Therefore, it is important to select an appropriate API solid state form for successful drug development. According to the Biopharmaceutical Classification System (BCS), ETZ was classified as a low solubility drug (BCS class II). Solubility can be enhanced either by salt formation or by cocrystal formation. The ETZ molecule does not have any ionization site for salt formation; therefore, improvement in the solubility of ETZ drug molecule can only be done by cocrystallization. The solubility of ETZ and ETA-2TMA·MeOH in  $37^\circ\text{C}$  water was determined. The results in Figure 5 clearly show that the solubility of ETA-2TMA·MeOH decreased to 19.30% of pure ETZ.

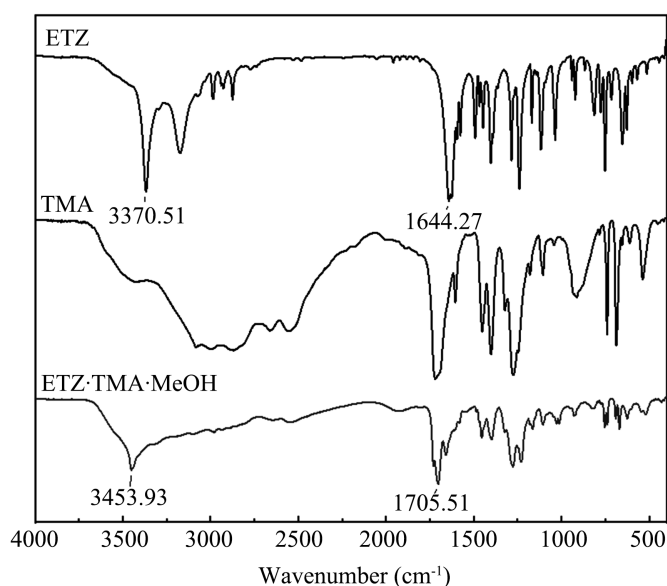


**Figure 4.** Comparison of FT-IR spectra of ETZ, TMA and ETA-2TMA·MeOH.

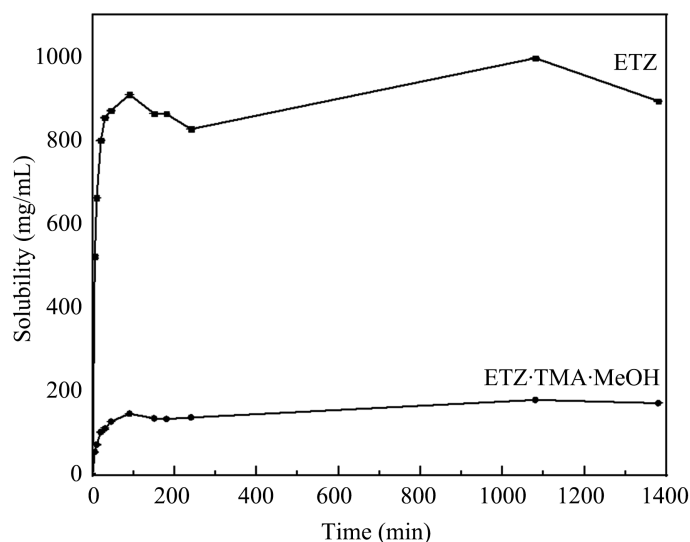


**Figure 5.** Solubility of ETZ and ETA-2TMA·MeOH in aqueous solution.

#### 4. Conclusion

ETA-2TMA·MeOH cocrystal was prepared by solution evaporation crystallization, and the cocrystal was characterized by SCXRD, PXRD and FT-IR. It was proved that 1 molecule ETZ, 2 molecule TMA and 1 molecule MeOH formed cocrystals by hydrogen bonding. The synthesis of the new cocrystal was confirmed by Fourier Transform Infrared and Powder X-ray Diffraction. The crystal structure of the ETA-2TMA·MeOH crystal was characterized by Single Crystal X-ray Diffractometer. In addition, the influence of cocrystallization on the solubility of ETZ was determined by HPLC. The results showed that the solubility of ETA-2TMA·MeOH decreased to 19.30% of pure ETZ. Its pharmacological and toxicological properties need further study.



## Conflicts of Interest

The authors declare no conflicts of interest.

## References

- [1] Ozawa, M., Hasegawa, K., Yonezawa, Y. and Sunada, H. (2002) Preparation of Solid Dispersion for Ethenzamide-Carbopol and Theophylline-Carbopol Systems Using a Twin Screw Extruder. *Chemical and Pharmaceutical Bulletin*, **50**, 802-807. <https://doi.org/10.1248/cpb.50.802>
- [2] Aitipamula, S., Chow, P.S. and Tan, R.B.H. (2010) Conformational and Enantiotropic Polymorphism of a 1:1 Cocrystal Involving Ethenzamide and Ethylmalonic Acid. *CrystEngComm*, **12**, 3691-3697. <https://doi.org/10.1039/c004491a>
- [3] Acebedo-Martínez, F.J., Alarcón-Payer, C., Rodríguez-Domingo, L., Domínguez-Martín, A. and Gómez-Morales, J. (2021) Furosemide/Non-Steroidal Anti-Inflammatory Drug-Drug Pharmaceutical Solids: Novel Opportunities in Drug Formulation. *Crystals*, **11**, 1339. <https://doi.org/10.3390/cryst11111339>
- [4] Nechipadappu, S.K. and Trivedi, D.R. (2018) Cocrystal of Nutraceutical Sinapic Acid with Active Pharmaceutical Ingredients Ethenzamide and 2-Chloro-4-Nitrobenzoic Acid: Equilibrium Solubility and Stability Study. *Journal of Molecular Structure*, **1171**, 898-905. <https://doi.org/10.1016/j.molstruc.2018.06.074>
- [5] Khatioda, R., Saikia, B., Das, P.J. and Sarma, B. (2017) Solubility and *in Vitro* Drug Permeation Behavior of Ethenzamide Cocrystals Regulated in Physiological PH Environments. *CrystEngComm*, **19**, 6992-7000. <https://doi.org/10.1039/C7CE01626C>
- [6] Potticary, J., Hall, C., Hamilton, V., Hamilton, V., McCabe, J.F. and Hall, S.R. (2020) Crystallization from Volatile Deep Eutectic Solvents. *Crystal Growth & Design*, **20**, 2877-2884. <https://doi.org/10.1021/acs.cgd.0c00399>
- [7] Aitipamula, S., Chow, P.S. and Tan, R.B.H. (2010) Polymorphs and Solvates of a Cocrystal Involving an Analgesic Drug, Ethenzamide, and 3, 5-Dinitrobenzoic Acid. *Crystal growth & design*, **10**, 2229-2238. <https://doi.org/10.1021/cg9015178>
- [8] Khatioda, R., Bora, P. and Sarma, B. (2018) Trimorphic Ethenzamide Cocrystal: *In Vitro* Solubility and Membrane Efflux Studies. *Crystal Growth & Design*, **18**, 4637-4645. <https://doi.org/10.1021/acs.cgd.8b00603>
- [9] Hariprasad, V.M., Nechipadappu, S.K. and Trivedi, D.R. (2016) Cocrystals of Ethenzamide: Study of Structural and Physicochemical Properties. *Crystal Growth & Design*, **16**, 4473-4481. <https://doi.org/10.1021/acs.cgd.6b00606>
- [10] Aitipamula, S., Wong, A.B.H., Chow, P.S. and Tan, R.B. (2012) Pharmaceutical Cocrystals of Ethenzamide: Structural, Solubility and Dissolution Studies. *CrystEngComm*, **14**, 8515-8524. <https://doi.org/10.1039/c2ce26325d>
- [11] Kozak, A., Marek, P.H. and Pindelska, E. (2019) Structural Characterization and Pharmaceutical Properties of Three Novel Cocrystals of Ethenzamide with Aliphatic Dicarboxylic Acids. *Journal of pharmaceutical sciences*, **108**, 1476-1485. <https://doi.org/10.1016/j.xphs.2018.10.060>
- [12] Nechipadappu, S.K., Tekuri, V. and Trivedi, D.R. (2017) Pharmaceutical Co-Crystal of Flufenamic Acid: Synthesis and Characterization of Two Novel Drug-Drug Co-Crystal. *Journal of Pharmaceutical Sciences*, **106**, 1384-1390. <https://doi.org/10.1016/j.xphs.2017.01.033>
- [13] Sarmah, K.K., Boro, K., Arhangelskis, M. and Thakuriaet, R. (2017) Crystal Structure Landscape of Ethenzamide: A Physicochemical Property Study. *CrystEngComm*,

**19**, 826-833. <https://doi.org/10.1039/C6CE02057G>

- [14] Aitipamula, S., Chow, P.S. and Tan, R.B.H. (2009) Dimorphs of a 1:1 Cocrystal of Ethenzamide and Saccharin: Solid-State Grinding Methods Result in Metastable Polymorph. *CrystEngComm*, **11**, 889-895. <https://doi.org/10.1039/b821373a>